AFRL-ML-WP-TP-2007-554

COMBINED NONLINEAR EFFECTS IN TWO-PHOTON ABSORPTION CHROMOPHORES AT HIGH INTENSITIES (POSTPRINT)

Richard L. Sutherland, Daniel G. McLean, Mark C. Brant, Joy E. Rogers, Paul A. Fleitz, and Augustine M. Urbas

Hardened Materials Branch
Survivability and Sensor Materials Division

AUGUST 2006

AIR FORCE RESEARCH LABORATORY
MATERIALS AND MANUFACTURING DIRECTORATE
WRIGHT-PATTERSON AIR FORCE BASE, OH 45433-7750
AIR FORCE MATERIEL COMMAND
UNITED STATES AIR FORCE

NOTICE AND SIGNATURE PAGE

Using Government drawings, specifications, or other data included in this document for any purpose other than Government procurement does not in any way obligate the U.S. Government. The fact that the Government formulated or supplied the drawings, specifications, or other data does not license the holder or any other person or corporation; or convey any rights or permission to manufacture, use, or sell any patented invention that may relate to them.

This report was cleared for public release by the Air Force Research Laboratory Wright Site (AFRL/WS) Public Affairs Office and is available to the general public, including foreign nationals. Copies may be obtained from the Defense Technical Information Center (DTIC) (http://www.dtic.mil).

AFRL-ML-WP-TP-2007-554 HAS BEEN REVIEWED AND IS APPROVED FOR PUBLICATION IN ACCORDANCE WITH ASSIGNED DISTRIBUTION STATEMENT.

*//Signature//

PAUL A. FLEITZ, Ph.D.
Program Manager
Exploratory Development
Hardened Materials Branch

//Signature//

MARK S. FORTE, Acting Chief
Hardened Materials Branch
Survivability and Sensor Materials Division

//Signature//

TIM J. SCHUMACHER, Chief
Survivability and Sensor Materials Division

This report is published in the interest of scientific and technical information exchange, and its publication does not constitute the Government's approval or disapproval of its ideas or findings.

*Disseminated copies will show "//Signature//" stamped or typed above the signature blocks.

REPORT DOCUMENTATION PAGE

Form Approved
OMB No. 0704-0188

1. REPORT DATE *(DD-MM-YY)*	2. REPORT TYPE	3. DATES COVERED *(From - To)*
August 2006	Conference Paper Postprint	

4. TITLE AND SUBTITLE
COMBINED NONLINEAR EFFECTS IN TWO-PHOTON ABSORPTION CHROMOPHORES AT HIGH INTENSITIES (POSTPRINT)

5a. CONTRACT NUMBER
In-house

5b. GRANT NUMBER

5c. PROGRAM ELEMENT NUMBER
62102F

6. AUTHOR(S)
Richard L. Sutherland, Daniel G. McLean, and Mark C. Brant (Science Applications International Corporation)
Joy E. Rogers (UES, Inc.)
Paul A. Fleitz and Augustine M. Urbas (AFRL/MLPJ)

5d. PROJECT NUMBER
4348

5e. TASK NUMBER
RG

5f. WORK UNIT NUMBER
M08R1000

7. PERFORMING ORGANIZATION NAME(S) AND ADDRESS(ES)
Science Applications International Corporation
Dayton, OH 45431

UES, Inc.
4401 Dayton-Xenia Road
Dayton, OH 45432

Hardened Materials Branch (AFRL/MLPJ)
Survivability and Sensor Materials Division
Materials and Manufacturing Directorate
Wright-Patterson Air Force Base, OH 45433-7750
Air Force Materiel Command
United States Air Force

8. PERFORMING ORGANIZATION REPORT NUMBER
AFRL-ML-WP-TP-2007-554

9. SPONSORING/MONITORING AGENCY NAME(S) AND ADDRESS(ES)
Air Force Research Laboratory
Materials and Manufacturing Directorate
Wright-Patterson Air Force Base, OH 45433-7750
Air Force Materiel Command, United States Air Force

10. SPONSORING/MONITORING AGENCY ACRONYM(S)
AFRL/MLPJ

11. SPONSORING/MONITORING AGENCY REPORT NUMBER(S)
AFRL-ML-WP-TP-2007-554

12. DISTRIBUTION/AVAILABILITY STATEMENT
Approved for public release; distribution unlimited.

13. SUPPLEMENTARY NOTES
Conference paper published in the Proceedings of SPIE, Vol. 6330, 2006. The U.S. Government is joint author of this work and has the right to use, modify, reproduce, release, perform, display, or disclose the work. PAO Case Number: AFRL/WS 06-1698, 10 Jul 2006.

14. ABSTRACT
Large two-photon and excited state absorption have been reported in donor-acceptor-substituted π-conjugated molecules. We have performed detailed nonlinear absorption and photophysical measurements on a system of AFX chromophores and calculate the nonlinear transmission based on an effective three-level model. A numerical model that includes far wing linear absorption has been developed and compared with an analytical three-photon absorption model. The models are in accordance and yield excellent agreement with experimental nonlinear transmission data for 0.02-M AFX solutions up to laser intensities ~ 1-5 GW/cm^2. We have extended our modeling efforts to include some new effects that may be anticipated in this regime, such as stimulated scattering, molecular interactions, and saturation. Effects of chirped pulses and linewidth of the pump laser on stimulated scattering are included. Self-focusing and de-focusing are also considered. We report on our experimental observations of various materials and discuss results with respect to our extended theoretical models.

15. SUBJECT TERMS
two-photon absorption, excited state absorption, nonlinear transmission, nonlinear scattering

16. SECURITY CLASSIFICATION OF:			17. LIMITATION OF ABSTRACT:	18. NUMBER OF PAGES	19a. NAME OF RESPONSIBLE PERSON (Monitor)
a. REPORT	b. ABSTRACT	c. THIS PAGE			Paul A. Fleitz
Unclassified	Unclassified	Unclassified	SAR	22	19b. TELEPHONE NUMBER *(Include Area Code)* N/A

Combined nonlinear effects in two-photon absorption chromophores at high intensities

R. L. Sutherland*[a], D. G. McLean[a], M. C. Brant[a], J. E. Rogers[b], P. A. Fleitz[c], and A. M. Urbas[c]
[a]Science Applications International Corporation, Dayton, OH, USA 45431
[b]UES, Inc., Dayton, OH, USA 45432
[c]Air Force Research Laboratory (AFRL/MLPJ), Wright-Patterson Air Force Base, OH, USA 45433

ABSTRACT

Large two-photon and excited state absorption have been reported in donor-acceptor-substituted π-conjugated molecules. We have performed detailed nonlinear absorption and photophysical measurements on a system of AFX chromophores and calculate the nonlinear transmission based on an effective three-level model. A numerical model that includes far wing linear absorption has been developed and compared with an analytical three-photon absorption model. The models are in accordance and yield excellent agreement with experimental nonlinear transmission data for 0.02-M AFX solutions up to laser intensities ~ 1-5 GW/cm^2. We have extended our modeling efforts to include some new effects that may be anticipated in this regime, such as stimulated scattering, molecular interactions, and saturation. Effects of chirped pulses and linewidth of the pump laser on stimulated scattering are included. Self-focusing and de-focusing are also considered. We report on our experimental observations of various materials and discuss results with respect to our extended theoretical models.

Keywords: two-photon absorption, excited state absorption, nonlinear transmission, nonlinear scattering

1. INTRODUCTION

Symmetric and asymmetric electron-donor/acceptor-substituted, π-conjugated systems are a major class of enhanced two-photon absorption (TPA) materials.[1,2] The molecular TPA cross section, σ_2, is often characterized by nonlinear transmittance (NLT) experiments, both in the nanosecond and femtosecond regimes. However, the nanosecond measurements in these materials typically yield values of σ_2 larger by more than two orders of magnitude.[3,4] Excited state absorption (ESA) has been postulated to play a role in the nanosecond measurements, and for this reason the nonlinear parameters have been called effective TPA cross sections.[5,6] Effective TPA cross sections are useful for screening nonlinear absorption (NLA) effectiveness of materials in the nanosecond regime. However, understanding the physics of nanosecond NLA is necessary for designing improved materials.

TPA followed by ESA was observed as early as 1974, and a value for the product of the ESA cross section and excited state lifetime of the chromophore was estimated based on a rate equation analysis.[7] Several authors have posited the effects of excited states on nonlinear absorption and refraction, and these effects have been convincingly demonstrated in degenerate four-wave mixing and Z-scan experiments.[8-11] Evidence of ESA has been demonstrated in NLT and Z-scan measurements of organic materials, and effective (intensity dependent) TPA coefficients have been employed to estimate ESA cross sections.[3,11] Recently, we have independently identified and characterized these excited states, then used this information to theoretically model nanosecond NLT measurements.[12,13] The nature of these excited states is important. For example, properties of the excited singlet state are significant for fluorescence imaging and laser applications, whereas the triplet state plays an important role in photopolymerization and photodynamic therapy. Moreover, the intrinsic (pulse-width independent) value of the TPA cross section σ_2 as well as the significance of ESA in comparison to other potential competing or contributing nonlinear mechanisms, such as stimulated scattering, self-focusing/defocusing, and quenching, need to be elucidated for accurate modeling of nonlinear absorption in the nanosecond regime. Accounting for these other phenomena as potential sources of NLT would enhance our understanding of the process in these chromophores.

*sutherlandr@saic.com

Nonlinear Optical Transmission and Multiphoton Processes in Organics IV,
edited by A. Todd Yeates, Kevin D. Belfield, Francois Kajzar, Proc. of SPIE Vol. 6330, 633006, (2006)
0277-786X/06/$15 · doi: 10.1117/12.679587

We have performed detailed nonlinear absorption and photophysical measurements on a system of AFX and similar chromophores and calculate the nonlinear transmission based on an effective three-level model. A numerical model that includes far wing linear absorption has also been developed and compared with the analytical three-photon absorption model. The presence of small, linear absorption may lead to a two-step, two-photon absorption process.[14] The models, however, are in accordance and yield close agreement with experimental nonlinear transmission data for 0.02-M AFX solutions up to laser intensities ~ 1-5 GW/cm^2. We have extended our modeling efforts to include some new effects that may be anticipated in this and higher intensity regimes, such as stimulated scattering, molecular interactions, and self-(de)focusing. We report here on these extensions to our models and discuss the effects these additional phenomena can be expected to have on NLT measurements.

2. MATERIALS

The chromophores used in this study are part of a class of TPA materials (designated AFX) having a design based on a push-pull charge-transfer model and multidimensional conjugation motif.[6] Examples of these molecules are given in an accompanying paper.[15] These molecules were synthesized and purified in the Polymer Branch of the Air Force Materials Directorate (AFRL/MLBP) as described in References 4, 6, and 22. Solutions of each were prepared in tetrahydrofuran (THF) for both photophysical characterization and NLT experiments.

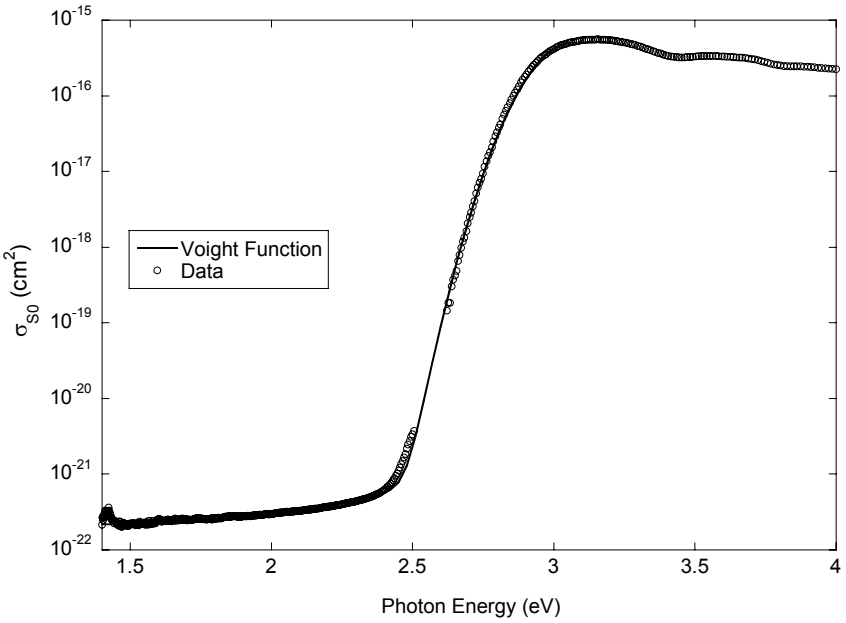

Figure 1. Linear absorption spectrum (ground state cross section σ_{S0}) of AF350 in THF. The circles are data and the curve is a Voigt function fit to the data. Spectra for other AFX molecules are similar.

A typical linear absorption spectrum is shown in Figure 1. The λ_{max} is in the UV or deep blue region of the visible spectrum, with absorption band edges ranging from ~ 450 nm to ~ 470 nm. In each case there is very little absorption ($\sigma_{S0} < 10^{-21}$ cm^2) in the 2.5-1.4 eV (500-900 nm) region. The purity should be at least 98% for glassy materials (e.g., AF455) and 99% for crystalline compounds (e.g., AF240) based on elemental analysis together with spectroscopic methods and melting point determination. There is only a single peak detected by liquid chromatography for materials such as AF350 and AF455. An impurity with a peak in the 500-900 nm range with a peak absorption cross section of $\geq 10^{-17}$ cm^{-2} would be observed at a fractional concentration of 10 ppm or less. We conclude that it is unlikely that there is significant impurity absorption in the samples.

3. THEORETICAL MODELS

3.1. Effective TPA and 3PA Models

Simple analytical models that can adequately explain and reliably predict the nanosecond NLT based on measurable properties of the chromophores and the laser pulse are desirable. The model we have developed for this purpose is similar to that used for reverse saturable absorption media, but with TPA from the ground state.[12] We consider ESA from the lowest lying singlet and triplet states. Two-photon-induced ESA is a three-photon process, although three photons are not absorbed simultaneously due to the finite lifetimes of the excited states. In the following we present an analytical model that incorporates these ideas as an effective three-photon absorption (3PA).[12]

We have for the spatial evolution of the intensity I,

$$\frac{\partial I}{\partial z} = -\left(\beta + \gamma_{\text{eff}} I\right) I^2 \tag{1}$$

where

$$\gamma_{\text{eff}} = \frac{\tau_p \sigma_{\text{eff}} \sigma_2 N}{2\hbar\omega}, \tag{2}$$

$$\sigma_{\text{eff}} = \eta\sigma_{S1} + \left(\tfrac{1}{2} - \eta\right)\varphi_T \sigma_{T1}, \tag{3}$$

$\beta = \sigma_2 N$ is the TPA coefficient, and $\eta = (\tau_S/\tau_p)\{1 - (\tau_S/\tau_p)[1 - \exp(-\tau_p/\tau_S)]\}$. We have thus modeled the system as a two-photon resonant, three-photon absorption medium, with an effective intermediate state that represents a time-averaged combination of the S_1 and T_1 states. Several authors have taken the quantity in parentheses in Eq. (1) to represent an effective TPA coefficient β_{eff}, from which an effective TPA cross section can be derived. We will consider both effective TPA and 3PA models in analyzing the experimental data. The quantity η is the pulse-averaged, relative weight of the S_1 state contribution to the effective ESA cross section. When $\tau_p << \tau_S$, $\eta \approx ½$ and ESA is essentially from the S_1 state only. On the other hand, when $\tau_p >> \tau_S$, $\eta \approx 0$ and all ESA is effectively from the T_1 state. When $\tau_p << \tau_S$, the growth of the S_1 population is linear, and the average growth time over a rectangular pulse is just $\tau_p/2$. The maximum relative weight of ½ for either state reflects the fact that in either time regime the growth rate of the respective excited state population (singlet or triplet) is approximately constant. The average population density over the entire pulse is then just one-half of the maximum density obtained at the end of the pulse, $N_{S1,\max} = \varphi_T^{-1} N_{T1,\max} = \tau_p \sigma_2 N I_{\text{peak}}^2 / 2\hbar\omega$. In an intermediate regime where $\tau_T >> \tau_p$ and $\tau_p \sim \tau_S$, $\eta < ½$ means that the S_1 population at the end of the pulse is smaller than $N_{S1,\max}$ because of continuous transitions to the S_0 and T_1 states as S_1 is being pumped, analogous to a leaky capacitor.

Equation (1) can be solved analytically, but the resulting expression is transcendental. However, if we take $\beta << \gamma_{\text{eff}} I$, the result reduces to a simple closed form identical to that for three-photon absorption. Assuming now Gaussian spatial and temporal profiles for the incident intensity, we integrate the resulting expression over space and time to obtain the energy transmittance for a sample of thickness d:

$$T = \frac{T_0^2}{\sqrt{\pi}\, p_0} \int_{-\infty}^{+\infty} \ln\left[\sqrt{1 + p_0^2 \exp\left(-2x^2\right)} + p_0 \exp\left(-x^2\right)\right] dx \tag{4}$$

where T_0 is the net linear transmittance from air into the medium due to Fresnel losses only (including all dielectric interfaces), $p_0 = (2\gamma_{\text{eff}} T_0^2 I_0^2 d)^{1/2}$, and I_0 is the incident peak, on-axis intensity. The parameters determining γ_{eff} can be found from femtosecond, picosecond, and nanosecond photophysical measurements and standard TPA measurements in the femtosecond regime.

For screening purposes it is often useful to define an effective TPA coefficient as above. The effective TPA cross section can be found by fitting the NLT data to the following equation:

$$T = \frac{T_0^2}{\sqrt{\pi} q_0} \int_{-\infty}^{\infty} \ln\left[1 + q_0 \exp\left(-x^2\right)\right] dx \tag{5}$$

where $q_0 = \beta_{eff} T_0 I_0 d$. The effective TPA cross section is then defined by $\sigma_{2eff} = \beta/N$.

3.2. Numerical ESA Model

The numerical model calculates the spatial, time, and radial dependence of three state populations; all of the transitions between these states; the bimolecular processes of triplet-triplet annihilation, ground state quenching, and oxygen quenching.[13] The radiation transport equation is then,

$$\frac{\partial I}{\partial z} = -\sigma_{S0} N_{S0} I - \sigma_2 N_{S0} I^2 - \sigma_{S1} N_{S1} I - \sigma_{T1} N_{T1} I \,. \tag{6}$$

The population rate equations are

$$\frac{\partial N_{S1}}{\partial t} = \frac{I}{\hbar\omega}\left(\sigma_{S0} + \frac{\sigma_2 I}{2}\right) N_{S0} - \frac{N_{S1}}{\tau_S} + \kappa_{TT} N_{T1}^2 \tag{7a}$$

$$\frac{\partial N_{T1}}{\partial t} = \frac{\varphi_T}{\tau_S} N_{S1} - \left(\frac{1}{\tau_T} + \kappa_{TT} N_{T1} + \kappa_{ST} N_{S0} + \kappa_{OT} N_O\right) N_{T1} \tag{7b}$$

$$\frac{\partial N_O}{\partial t} = -\kappa_{OT} N_O N_{T1} + k_O\left(N_O^0 - N_O\right) \tag{7c}$$

$$N_{S0} = N - N_{S1} - N_{T1} \,. \tag{7d}$$

where κ_{TT}, κ_{ST}, κ_{OT}, N_O, k_O are the triplet-triplet annihilation rate, the ground state self quenching rate of the triplet state, the oxygen quenching rate of the triplet state, the oxygen concentration, and the oxygen singlet state relaxation rate respectively. The rate equations are solved at every time step using a stiff Runge-Kutta algorithm supplied in MathCad. These populations are used to calculate the change in the intensity, which is then rescaled assuming Gaussian beam propagation at each z step. A range of input intensities are calculated and used to calculate both the NLT variation and the radial dependence. A Gaussian time profile is used. The radial and temporal integrations are performed to yield transmitted pulse energy. A normal reflection Fresnel loss is imposed on the incident intensity and again on the output intensity.

3.3. Stimulated Scattering Model

Recently, He et al. reported the observation of stimulated backscattering in a two-photon absorption medium, where the frequency of the stimulated wave was identical to the incident laser frequency, and the small-signal gain was quadratic in the incident laser intensity.[16,17] They considered a stimulated thermal Rayleigh scattering model based on TPA-enhanced temperature and density fluctuations, but ruled this out due to (a) the broad linewidth of their pump laser, which would severely reduce the gain of the stimulated wave, and (b) the fact that the peak gain in this theory is for an anti-Stokes-shifted wave, contrary to their experimental results. They concluded that the stimulated wave was due to a Bragg grating formed by the superposition of the incident laser beam and an elastically (Rayleigh) backscattered wave, creating an index grating via a TPA-resonance enhanced nonlinear index coefficient n_2. The stimulated backscattered wave is then due to reflection of the laser from this grating.

Two-beam coupling (TBC) has a rich history in nonlinear optics. Early studies by Silberberg and Bar Joseph established two conditions for one-way energy transfer between waves in a Kerr medium: 1) the frequencies must be nondegenerate, and 2) the nonlinearity must have a finite response time.[18] For a positive Kerr nonlinearity energy transfer under these conditions is always from the high frequency to low frequency beam. Yeh later gave an exact solution for energy

transfer between two co-propagating beams including the effect of linear absorption.[20] In each of these studies, both beams had non-zero input values.

TBC also describes several stimulated scattering phenomena, such as stimulated Raman (SRS), Brillouin (SBS), and Rayleigh-wing scattering (SRWS), where one beam is derived internally from the incident laser. For example, the Stokes wave in these phenomena arises internally from scattered light and experiences gain at the expense of the incident laser beam. In each of these stimulated scattering effects the small-signal gain of the Stokes wave is proportional to the laser intensity, not the square of the intensity.[21]

The model proposed by He et al. would thus appear to violate the two conditions previously established for one-way energy transfer by TBC in a Kerr medium: the frequencies of the two beams are not different, and the third order susceptibility related to TPA, due to an electronic polarization, has a virtually instantaneous response for nanosecond laser pulses.

In Ref. 23 Sutherland considered a field with a time dependent amplitude and phase, $E(t) \sim A(t)\exp[-i\varphi(t)]$. A Taylor series expansion of the phase yields (ignoring a constant term) $\varphi(t) = \omega t + bt^2 + \ldots$, where ω is the central frequency of the wave, and b is a linear chirp coefficient. For simplicity, higher order terms were ignored.

Let the total field in a medium of length d be described by

$$\begin{aligned} E(z,t) = {} & A_L(z, t+\tau)\exp\left\{ i[kz - \omega t - b(t+\tau)^2] \right\} \\ & + A_S(z, t-\tau)\exp\left\{ i[-kz - \omega t - b(t-\tau)^2] \right\} + c.c. \end{aligned} \tag{8}$$

where $k = n\omega/c$, n is the linear refractive index, and $2\tau = 2n(d - z)/c$ is the relative time delay at position z and time t between the forward propagating laser wave (L) and the backward propagating scattered wave (S). We assume that the scattered wave originates at $z = d$ by some elastic scattering process, so $A_S(d,t) = \sqrt{\eta} A_L(d,t)$ where η is a constant << 1. Consequently, the scattered wave has the same spectral composition as the incident laser wave. However, for $z \neq d$ a lower frequency part of the scattered wave is always interacting with a higher frequency part of the incident wave. The total polarization of the medium is given by

$$P = \varepsilon_0 \left(\chi_g^{(1)} + (N_e/N)\Delta\chi^{(1)} + 3\chi^{(3)} \left\langle E^2 \right\rangle \right) E \tag{9}$$

where $\chi^{(n)}$ is the n-th order susceptibility, and the angular brackets indicate an average over a time longer than an optical period but shorter than $(2b\tau)^{-1}$. We have assumed that TPA produces a single excited state of number density $N_e << N$, the total number density of the nonlinear chromophore. Both $\Delta\chi^{(1)} = \chi_e^{(1)} - \chi_g^{(1)}$ and $\chi^{(3)}$ are complex quantities (g signifies the ground state of the medium). The population of the state excited by TPA decays back to the ground state with a time constant T_e, so N_e obeys the following kinetic equation:

$$\frac{\partial N_e}{\partial t} = \frac{\sigma_2 N I^2}{2\hbar\omega} - \frac{N_e}{T_e} \tag{10}$$

where $I(z,t) = 2\varepsilon_0 nc\left\langle E^2(z,t) \right\rangle$ is the total intensity. Let the amplitudes be slowly varying in time compared to T_e. Equation (10) can then be integrated to yield

$$N_e/N = C_0 + \{C_1 \exp[i(2kz - 4b\tau)] + C_2 \exp[i(4kz - 8b\tau)] + c.c.\}, \tag{11a}$$

$$C_0 = \frac{\sigma_2 T_e}{2\hbar\omega}\left(I_L^2 + I_S^2 + 4 I_L I_S \right), \tag{11b}$$

$$C_1 = \frac{\sigma_2 T_e}{2\hbar\omega}(I_L + I_S)\left(\frac{4\varepsilon_0 ncA_L A_S^*}{1 - i4b\tau T_e} \right), \tag{11c}$$

$$C_2 = \frac{\sigma_2 T_e}{2\hbar\omega} \frac{\left(2\varepsilon_0 ncA_L A_S^*\right)^2}{1 - i8b\tau T_e}, \tag{11d}$$

where ε_0 is the free-space permittivity. We will make the assumption that $(4b\tau T_e)^2 << 1$.

Following a procedure directly analogous to that of Yeh[20] and Boyd[21] for non-degenerate TBC, Eqs. (11a)-(11d) are substituted into Eq. (9), and then both Eqs. (8) and (9) are substituted into Maxwell's wave equation in the slowly varying amplitude approximation. Matching up synchronous terms, the following coupled-wave equations for the laser and backscattered intensities are derived:

$$\frac{dI_L}{dz} = -g(1-z/d)(I_L + I_S)I_L I_S - \gamma_{eff}\left(I_L^2 + 3I_S^2 + 6I_L I_S\right)I_L - \beta(I_L + 2I_S)I_L \tag{12a}$$

$$\frac{dI_S}{dz} = -g(1-z/d)(I_L + I_S)I_L I_S + \gamma_{eff}\left(3I_L^2 + I_S^2 + 6I_L I_S\right)I_S + \beta(2I_L + I_S)I_S \tag{12b}$$

where g and γ_{eff} are the backward wave gain and effective three-photon absorption (3PA) coefficients, respectively, with

$$g = \frac{8bT_e\omega\Delta\chi_R^{(1)}d}{c^2 I_{sat}^2}, \tag{13}$$

$$\gamma_{eff} = \frac{N\Delta\sigma}{I_{sat}^2}, \tag{14}$$

where $\Delta\chi_R^{(1)} = \mathrm{Re}\left(\Delta\chi^{(1)}\right)$, $\Delta\sigma = \sigma_e - \sigma_g$ is the difference between the linear absorption cross sections of the excited and ground states, and $I_{sat} = \left(2\hbar\omega/\sigma_2 T_e\right)^{1/2}$ is the two-photon saturation intensity. Note the similarity between Eqs. (14) and (2).

Linear chirp is not a unique requirement for the energy transfer between incident laser and elastically backscattered waves. Another potential mechanism involves multimode beams. Take the simple case where the incident laser wave consists of two modes: ω_0 and $\omega_1 = \omega_0 + \delta\omega > \omega_0$ ($\delta\omega << \omega_0$). Here the modes are not in any time-ordered sequence (such as a chirp, where the frequency varies linearly in time), and can thus interact simultaneously through the nonlinear polarization of the medium over the duration of the pulse. Employing the mechanism involving a TPA-populated excited state described above, there will be energy transfer from the ω_1 mode of the incident laser beam to the ω_0 mode of the backscattered beam.[21] Likewise, the ω_1 mode of the backscattered wave will yield its energy to the ω_0 mode of the laser wave. Thus, we need consider only coupling between the laser frequency at ω_1 with the backscattered wave at ω_0. In this case the above formalism may be used with the substitution $4b\tau \rightarrow \delta\omega$.

3.4. Nonlinear Beam Propagation Model

To incorporate the effects of nonlinear focusing on the NLT, we must solve the full three-dimensional wave equation in the slowly varying amplitude approximation. The solution for the amplitude after propagation through a small distance Δz along the z-axis can be written formally as[24,25]

$$A(r, z+\Delta z) = \exp\left(i\frac{\Delta z}{2k}H\right)A(r,z) \tag{15}$$

where H is an operator containing radial and nonlinear dependence of the beam propagation. We assume the beam has axial symmetry. Thus,

$$H = \frac{\partial^2}{\partial r^2} + \frac{1}{r}\frac{\partial}{\partial r} + f\left(AA^*\right). \tag{16}$$

The function f contains the nonlinear terms of the wave equation. In an isotropic system, this will include only odd-order nonlinear susceptibility terms. To third order, it will include the effects of nonlinear refraction and TPA. We wish to also incorporate the effect of excited state absorption through the effective 3PA approach. Hence, the nonlinear function in Eq. (16) becomes

$$f = \left(\frac{8n\pi^2 n_2}{\lambda^2} + i\frac{2\pi n\beta}{\lambda} + i\frac{4\pi\gamma_{eff}}{n\lambda} AA^* \right) AA^*, \tag{17}$$

where n_2 is the nonlinear refractive index coefficient in intensity units (cm^2/W).

We used the technique of Feit and Fleck[24] to solve the wave equation, which involves expanding the exponential operator of Eq. (15) in a Taylor series and applying the operators term by term on the wave amplitude $A(r,z)$. The radial derivatives are found by writing the wave amplitude as a digital Fourier series and using fast Fourier transform algorithms. The input amplitude is taken to be a focused Gaussian beam with the waist in the center of the sample. For free-space propagation, we kept terms to second order in the expansion of Eq. (15). We checked the accuracy of this approach by computing the linear propagation of a focused Gaussian beam and comparing it to the analytical result. Agreement was better than 1% when including terms to second order.

4. EXPERIMENTAL

Micromolar solutions were prepared for conventional photophysical measurements (lifetimes, excited state cross sections, and quantum yields). Details of these experiments can be found elsewhere.[26] All solution samples for nanosecond NLT measurements had concentrations of 0.02 M (mol/L) and were placed in 1-mm glass or fused silica cuvettes. Intrinsic σ_2 values were obtained from independent femtosecond measurements.[12]

Nanosecond nonlinear transmittance measurements were performed with a Nd:YAG pumped optical parametric oscillator (OPO) tuned from 660 to 880 nm. The pulse was Gaussian shaped with τ_L = 3.5 ns. The beam was focused with an f = 50-cm lens into the sample. Over the length of the sample (1 mm) the beam was essentially collimated. The beam shape was slightly elliptical, with a geometric-mean $1/e^2$ radius $w \approx 18.4 - 18.9$ μm, assuming an approximately Gaussian beam shape. The energy was varied, and incident and transmitted energies were measured with energy meters. To rule out the effects of output beam spreading on transmittance measurements, a large-area (~ 1 cm^2) detector was placed near the exit of the sample to collect all transmitted energy. We also looked for stimulated backscattering by rotating the sample slightly to avoid Fresnel reflected light and measuring 180°-scattered light with an energy meter.

Intermolecular quenching properties were examined for AF350 and AF455. The ground state concentration was varied from 10 μM to 20 mM, and the triplet state lifetime measured. At ~ 10 μM the lifetime of AF350 was 182 μs under deoxygenated conditions, and the lifetime was 96 μs at 20 mM. A bimolecular self-quenching rate constant of 2×10^2 L/mol-s was measured. In addition, we have measured the triplet-triplet quenching rate in AF455 to be $\kappa_{TT} = 2.1 \times 10^9$ L/mol-s. Thus it appears that triplet-triplet annihilation is much more significant than self-quenching in these systems. However, the triplet yield in these systems is low. Based on an analysis of population kinetics, we would expect that $N_T < 0.1N$ even at the highest input energies. This would yield a rate $\kappa_{TT}N_T < 4 \times 10^6$ s^{-1} as an upper limit for triplet quenching, which is of the order of the phosphorescent rate. Since this implies a triplet lifetime long compared to the laser pulse, and since the dominant contribution to ESA appears to be from the S_1 state, we conclude that triplet quenching processes have no significant effect on the measured NLT in these AFX systems.

5. RESULTS AND DISCUSSION

5.1. TPA/ESA

A common method in the literature for screening TPA materials in the nanosecond regime is to fit the NLT data to a TPA transmittance (see Eq. (5)) and extract an effective TPA cross section. We give the results of such fits for two series of dipolar (AF240 and AF270), quadrupolar (AF287 and AF295), and octupolar (AF350 and AF380) molecules in Table 1. Effective σ_2 as a function of wavelength for a related chromophore (E1-BTF) is shown in Figure 2. E1-BTF is related to AF287, but has a platinum core bridging the two benzothiolazole fluorine arms.[15] Data such as these are useful for observing trends in molecular structure, but do not yield sufficient information to give directions for further improvement. For example, a large effective σ_2 could be due to a large intrinsic σ_2, a large singlet and/or triplet cross section, and/or a large triplet yield, or perhaps some other not yet recognized nonlinear effect. Hence, these NLT measurements must be supplemented with photophysical measurements. Both effective 3PA and numerical ESA models may then be applied to ascertain the quality of the model in reproducing the NLT results.

Table 1. Effective TPA Cross Sections of a Series of AFX Chromophores

Material	Effective σ_2 (10^{-20} cm^4/GW)
AF240	50
AF287	99
AF380	114
AF270	29
AF295	78
AF350	139

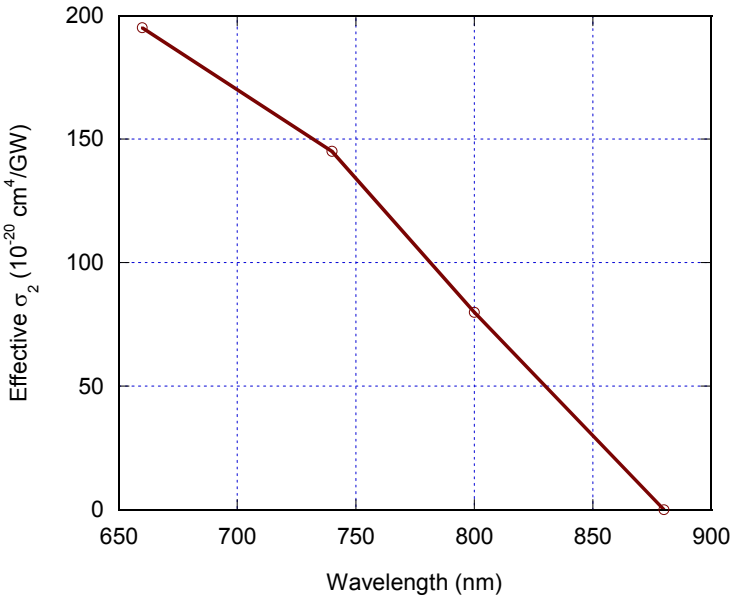

Figure 2. Effective TPA cross sections of E1-BTF measured with nanosecond laser pulses.

Photophysical data at 800 nm for this set of AFX chromophores, as well as data for AF455 at various wavelengths, are presented in Table 2. Using these data, and no adjustable parameters, we compute the expected transmittance of solutions in THF, based on Eqs. (2)-(4) and compare these to experimental nanosecond NLT data in Figure 3. For all of the solutions in these plots, the concentration is nominally 0.02 M with the exception of AF287, which is approximately 0.01 M due to solubility limitations. We can immediately see that, although the model predicts the general trends in the general pulse energy regime, the quantitative agreement with the data is not good in all cases. This is particularly surprising for AF240 and AF350 for which we obtained much better agreement between theory and data at 820 nm. Before addressing other possible nonlinearities contributing to this discrepancy, we should point out that for each of these molecules the triplet yield is very low, and thus the excited singlet-singlet absorption is playing a major role in the ESA. Excited state cross sections in the 800 nm regime are difficult to measure because this is the fundamental wavelength of the Ti:sapphire laser used in the experiments. A cutoff filter is used to eliminate this signal, making the measured absorbance signals at this wavelength somewhat noisy. The signals for shorter wavelengths do not have this problem. For example, we show in Figure 4 transmittance data and model results for AF455 at wavelengths of 740, 780, and 800 nm. The agreement between theory and data is very good. We conclude that the accurate measurement of the excited state

cross section σ_{S1} is crucial for these AFX chromophores, and measurements near the fundamental wavelength of the laser (800 nm) need to be improved.

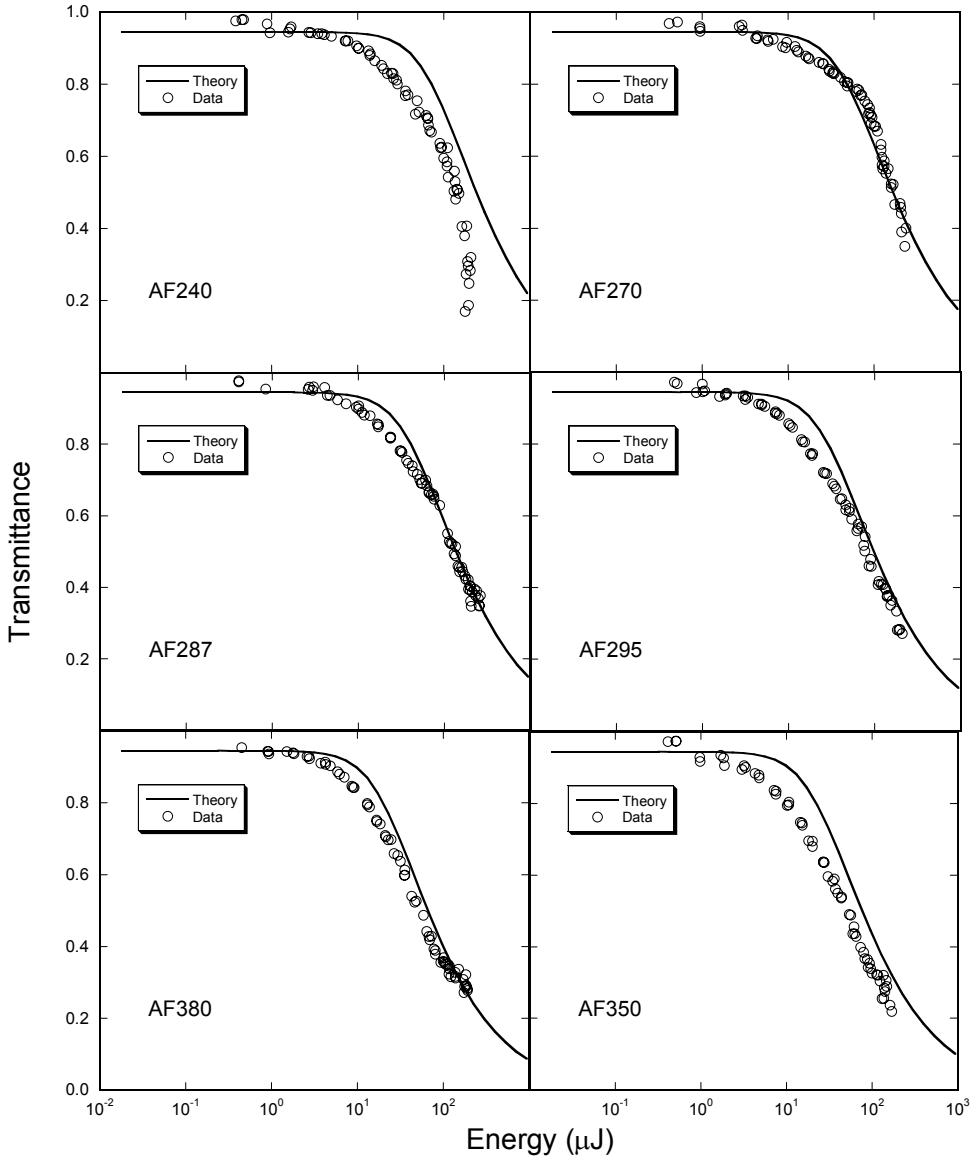

Figure 3. Nanosecond NLT data and model results for six AFX chromophores.

A closer examination of the plots in Figures 3 and 4 reveals that there are also some differences in the shape of the transmittance curves between theory and data. This is not so surprising at the highest pulse energies where it is conceivable that higher order nonlinearities may be evident, but there is also a consistent overestimation of the transmittance by the theory in the lower energy region where this measurement just begins to roll over with energy. Although this discrepancy is reasonably small and somewhat amplified due to the semi-log nature of the plot, it appears to be systematic and may suggest the presence of other nonlinearities that could possibly play a significant role as the pulse energy increases. One could question the nature of the approximations leading to the analytical effective 3PA model, but the close agreement between this analytical result and a finite difference numerical calculation of TPA followed by ESA (i.e., including detailed time-dependent behavior of singlet and triplet populations and pulse intensity absorption) indicates that the analytical approach is quite adequate for modeling these nonlinear effects.[12] Independent verification of this agreement with a generalized theoretical treatment of laser pulses interacting with multi-photon absorbers strength-

ens this conclusion.[27] We note that a two-step TPA mechanism (similar to reverse saturable absorption) has been proposed to explain the NLT in these types of chromophores,[14] and we have performed sensitive measurements of the linear absorption cross section in AF240, AF350, and AF455. Including the effects of these small measured ground state cross sections on the nonlinear absorption (and population kinetics), however, makes only very small corrections to the effective 3PA theory[13] and does not account for the discrepancies observed in the data. We conclude that the analytical effective 3PA result yields excellent quantitative predictions for the specific model in question, which is TPA followed by ESA from the singlet and triplet manifolds of the molecules. Therefore, we must look at potential alternative processes that may be at work in conjunction with TPA/ESA.

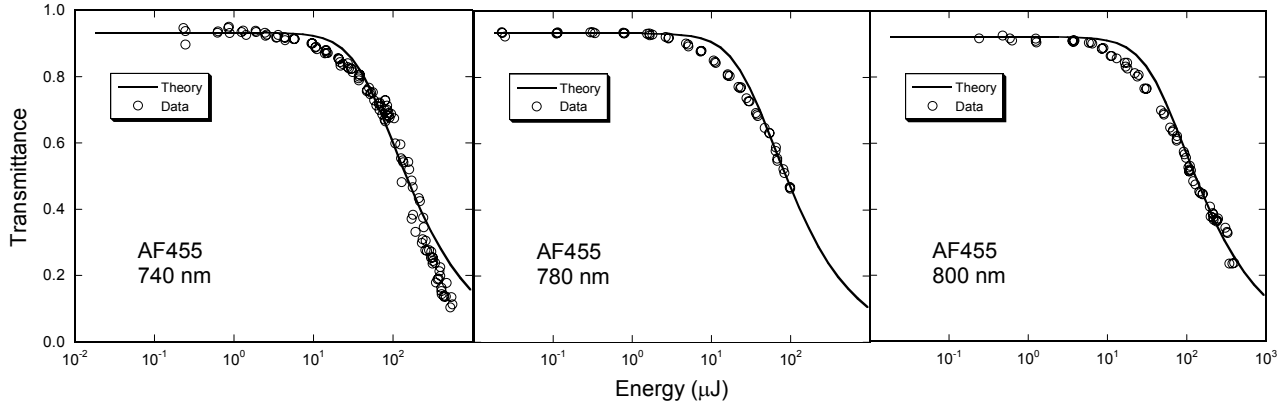

Figure 4. NLT data and model results for AF455 at three different wavelengths.

Table 2. Photophysical Properties of Various AFX Chromophores

Chromophore	Wavelength (nm)	σ_2 (10^{-20} cm^4/GW)	σ_{S1} (10^{-17} cm^2)	σ_{T1} (10^{-17} cm^2)	φ_T	τ_S (ns)
AF240	800	0.19	1.45	7.45	0.064	2.03
AF287	800	0.50	4.39	15.9	0.074	1.88
AF380	800	0.63	6.08	17.2	0.130	1.85
AF270	800	0.15	4.93	15.3	0.031	1.89
AF295	800	0.32	5.80	16.6	0.050	1.88
AF350	800	0.49	6.91	22.0	0.035	1.99
AF455	740	0.37	1.91	9.98	0.060	2.72
AF455	780	0.81	1.87	14.7	0.060	2.72
AF455	800	0.51	1.45	18.1	0.060	2.72

5.2. Stimulated Scattering

It is interesting that an effective TPA theory fits the data better in this low energy regime, indicating that some mechanism that has a quadratic intensity dependence may be at play. He et al.[17] have observed this kind of dependence and have verified in their case that this is due to a stimulated scattering phenomenon. We consider this next.

Let us examine Eqs. (12a) and (12b) for nonlinear scattering in the case when $I_S << I_L \approx$ constant. It can be seen that the backward stimulated wave will experience exponential growth when $I_L > 2\beta \Big/ \left(\frac{1}{2} g - 3\gamma_{eff}\right)$. This defines the threshold condition for stimulated backscattering when there is no linear absorption. From Eq. (12b), the small signal gain G, given in terms of $\Delta I_S = I_S(0) - I_S(d)$, is $G = \Delta I_S / I_S(d) \propto I_L^2$ for input intensities where the gain dominates TPA. Also, the reflectance of the scattered wave is defined by $R = I_S(0) / I_L(0)$, and the change

$\Delta R = R - \eta = \Delta I_S / I_L \propto I_S(d) I_L \propto G I_S(d) / I_L$. These results are in agreement with the data presented by He et al. for the measured small-signal gain and reflectance in a 0.01-M solution of PRL 802 in THF.[17]

Under conditions where the nonlinear absorption terms (β and γ_{eff}) can be ignored, i.e., where these loss terms are small compared to the TBC gain, Eqs. (12a) and (12b) can be solved analytically. The result can be expressed as

$$\eta_0 = \frac{R\left[(1-R)(1-R+3\eta_0)+2\eta_0^2\right]^{1/2}}{(1+R)^2 \exp(\Gamma)} \left(\frac{1-R+2\eta_0}{1-R+\eta_0}\right)^{3/2}, \tag{18}$$

where $\eta_0 = I_S(d)/I_L(0)$, and

$$\Gamma = \tfrac{1}{2}(1-R)^2 g I_L^2(0) d. \tag{19}$$

Note that in general $\eta_0 \neq \eta$, although when the gain is sufficiently small $\eta_0 \approx \eta$. Also, when the gain is not too large so that $(1 - R) >> \eta_0$, Eq. (18) can be simplified to the following approximation:

$$\eta_0 \approx \frac{R(1-R)}{(1+R)^2 \exp(\Gamma)}. \tag{20}$$

It is interesting to compare this result to the case of SBS, for which the denominator of Eq. (20) becomes $\exp(\Gamma) - R$ with $\Gamma \to (1-R) g_B I_L(0) d$, where g_B is the Brillouin gain coefficient.[21] Thus, in the case of negligible loss by absorption, the backscattered reflectance as a function of incident laser intensity will look similar to the Brillouin reflectance. A plot of the reflectance given by Eq. (20) for a constant input $I_S(d)/I_L(0)$, over a range of Γ where the approximation is valid, is shown in Figure 5.

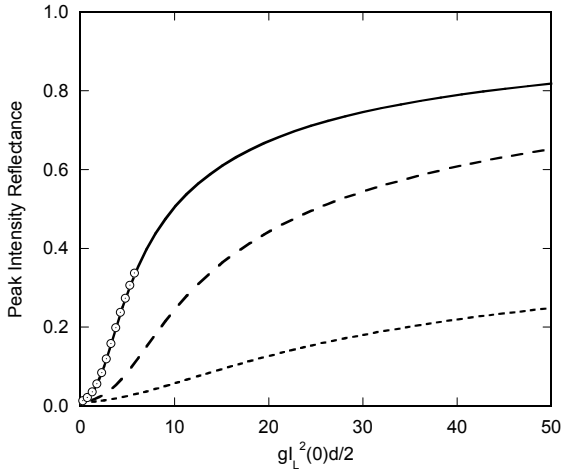

Figure 5. Backscattered reflectance vs. exponential gain factor. $\beta = 0$, $\gamma_{eff} = 0$ (solid); $g = 20\beta^2 d$, $\gamma_{eff} = 0$ (long dash); $g = 20\beta^2 d$, $g = 15\ \gamma_{eff}$ (short dash). Circles give R calculated by analytical approximation.

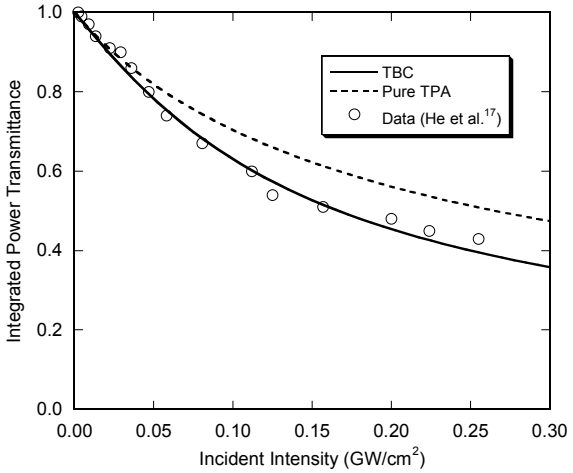

Figure 6. Nonlinear transmittance vs. incident intensity. Pure TPA, $\beta = 9.46$ cm/GW (dashed); $\beta = 9.46$ cm/GW, $g = 1800$ cm^3/GW^2, $\gamma_{eff} = 120$ cm^2/GW^2, $\eta = 0.04$ (solid). Circles are data according to He et al.[17]

Numerical solutions of Eqs. (12a) and (12b) are also given in Figure 5. These illustrate the agreement of the approximation given by Eq. (20) with the exact result, and the effect of including the nonlinear absorption terms. Figure 6 gives the laser transmittance. Parameters have been adjusted to yield results close to the experimental data of He et al.[16,17] The coefficients used are $\beta = 9.46$ cm/GW (the value quoted in Ref. 17), $\eta = 0.04$, $g = 1800$ cm^3/GW^2, and $\gamma_{eff} = 120$ cm^3/GW^2, with $d = 1$ cm. Here the transmittance is the ratio of output power to input power. To compute this, we assumed a Gaussian dependence for the input intensity and then integrated the output intensity over the area of the cylindrically symmetric beam. The result is compared with what would be expected for pure TPA (no TBC or ESA). The departure from pure TPA in this case is due primarily to energy transfer from the laser to the backscattered beam. A comparison with the data given in Ref. 17 shows good agreement with the results of this model.

To get an order of magnitude of the numbers involved, consider the experiment of He et al.[16,17] and the results shown in Figure 6. For a laser wavelength of 532 nm and $T_e \sim 1$ ns,[5,26] $I_{sat} \sim 0.7$ GW/cm^2. For a severely chirped pulse the laser linewidth is $\Delta\omega_L \sim 2b\tau_L$ where τ_L is the laser pulse width. For $\Delta\omega_L/2\pi \sim 24$ GHz (0.8 cm^{-1}), $\tau_L \sim 10$ ns, and $N = 6 \times 10^{18}$ cm^{-3} (0.01-M concentration), Eqs. (13) and (14) yield $\Delta\chi_R^{(1)} \sim 4 \times 10^{-3}$ and $\Delta\sigma \sim 1 \times 10^{-17}$ cm^2. These values yield approximate agreement with typical photophysical data for TPA chromophores, and thus suggests that this stimulated scattering with a quadratic intensity dependence may be contributing to the overall shape of the NLT curve.

Notice that $\mathrm{Re}\left(\chi^{(3)}\right)$, or n_2, does not appear in the gain coefficient of Eq. (13). The reason for this is that $\chi^{(3)}$ was assumed to have an instantaneous response [$\mathrm{Im}\left(\chi^{(3)}\right) \propto \beta$]. There is no two-beam coupling in a Kerr medium with an instantaneous response.[20,21] It is possible however, under TPA resonant conditions, that n_2 could have a finite response time (i.e., $\chi^{(3)}$ is complex with a finite damping coefficient[21]). However, if this is included in the development of the coupled-wave intensity equations, it would lead to a term in the gain G that is proportional to I_L, not I_L^2, which would be inconsistent with the experimental results of He et al.[17] It is also quite likely that the Kerr refractive term would be much smaller than the term proportional to $\Delta\chi_R^{(1)}$.

As noted earlier, the same theory just described can be applied to multimode pulses instead of chirped pulses with the simple substitution $4b\tau \rightarrow \delta\omega$. Pulses described in Ref. 17 appear to be multimode. However, as argued earlier the selective sign of the TBC gain would then cause only one mode of the backscattered wave to be amplified (assuming the laser oscillates on only two modes), thus making the backscattered pulse single mode. This appears not to be the case experimentally.[17] It seems likely that the laser pulse can be both multimode and chirped and thus produce a backscattered wave in accordance with experiment.

Applying this model to our experimental data appears to lead to a null result. We have looked for stimulated backscattering by rotating the sample slightly to avoid Fresnel reflected light and measuring 180°-scattered light with an energy meter. For example, at an incident pulse energy of 124 μJ on a sample of 0.02-M AF455 in THF, we measured ~ 2 nJ of backscattered light. This would correspond to $< 2 \times 10^{-5}$ efficiency for stimulated scattering, which can be considered negligible compared to the nonlinear absorption loss. To date, we have not observed any significant backscattered signal in our NLT experiments. The reasons for this are probably related to the nature of the input pulses. Whereas Ref. 17 used a Q-switched, frequency-doubled Nd:YAG laser as the input, we use a tunable OPO. The OPO is pumped by a seeded, single longitudinal mode Nd:YAG laser, and the OPO pulse shows no evidence of multimode behavior. Although the pump laser pulse may have some chirp due to the Q-switch, the bandwidth of the OPO pulse is dominated by angle phase matching effects. In fact, the bandwidth of the pulse is so large that the pulse should have a small coherence length. Indeed, measurements of the bandwidth at 800 nm (~ 37 cm^{-1}) indicate a theoretical coherence length of only ~ 270 μm. This is in rough agreement with the loss of fringe visibility in our experiments when the beam is split and propagated over a path difference of only ~ 100-200 μm. This is small compared to our sample thickness of 1 mm, and hence implies that the beam cannot interact via a Bragg grating coherently over a distance equal to the sample thickness. We conclude that stimulated backscattering, of the type observed by He et al. where the interaction length is a factor ~ 100× larger than our coherence length, is probably not making a substantial contribution to the NLT measurements in our experiments due to the nature of the OPO pulse.

5.3. Nonlinear Refraction Effects

The usual assumption in the modeling of nonlinear absorption is that the beam does not diffract significantly during its propagation through the sample. In other words, we assume that the only thing that can change the local intensity is absorption. However, since nonlinear absorption is intensity dependent, any nonlinear process that could affect the local intensity will in turn modify the nonlinear absorption. In a NLT experiment, we normally design the experiment so that self-(de)focusing effects do not lead to any loss in the *transmitted* (far field) beam. Nonlinear refraction can, however, also affect the local intensity in the sample and thus influence the nonlinear absorption. To study these effects, we have employed the nonlinear beam propagation model which includes diffraction and nonlinear refraction.

We consider a hypothetical material that has all of the photophysical properties of AF455, but for which we may vary the nonlinear refractive index coefficient, n_2. As described in Section 3.4, we include both TPA and the effective 3PA model. We take the input wave to the sample to be a focused Gaussian beam which has its waist (for the linear regime) located at the center of the sample. The Rayleigh range of the beam is longer than half the sample length. For the spe-

cific example considered here, we take the beam waist to have a radius w = 18 μm. The wavelength is 800 nm, and the sample is 1 mm thick. For purposes of calculating radial derivatives using the fast Fourier transform technique, we divided the beam radially into 128 equal increments and selected a total radial range of 78 μm. The integration step along the beam axis was chosen to be $\Delta z = 0.05\lambda$ = 0.04 μm. The output intensity was computed from the output field amplitude and then integrated radially, assuming axial symmetry, to compute the total integrated optical power.

Results of the calculation are shown in Figure 7, which plots the integrated power transmittance as a function of incident on-axis intensity (i.e., the peak intensity the beam would have at focus in a linear medium). The solid curve is the result of the effective 3PA model, which assumes that the beam, in the linear regime (low power), has a constant radius throughout the sample. The circles are the results of the nonlinear beam propagation model for $n_2 = 0$, i.e., negligible nonlinear refraction. Note that at high intensities these points lie just slightly above the curve for the analytical model. This is not an error due to the numerical calculations, but is due to the fact that the beam propagation model includes the effects of diffraction: the on-axis intensity is slightly reduced on either side of the focal region due to beam spreading, whereas the analytical model assumes constant beam radius. The squares give the NLT that would be measured if the sample has an n_2 equal to that of carbon disulfide. Self-focusing obviously increases the nonlinear absorption, but the variation is small and probably within typical measurement uncertainty. On the other hand, a negative index such as might be associated with a thermal nonlinearity, has a definite impact on the transmittance at higher intensity. Since the medium becomes more absorbing at high intensities, some of this energy is likely to be dissipated as heat and cause the beam to be thermally bloomed to some degree. This would increase the NLT and make it appear that the sample has smaller TPA and/or ESA cross sections. A rather large positive n_2 can make the NLT depart significantly from the ana-

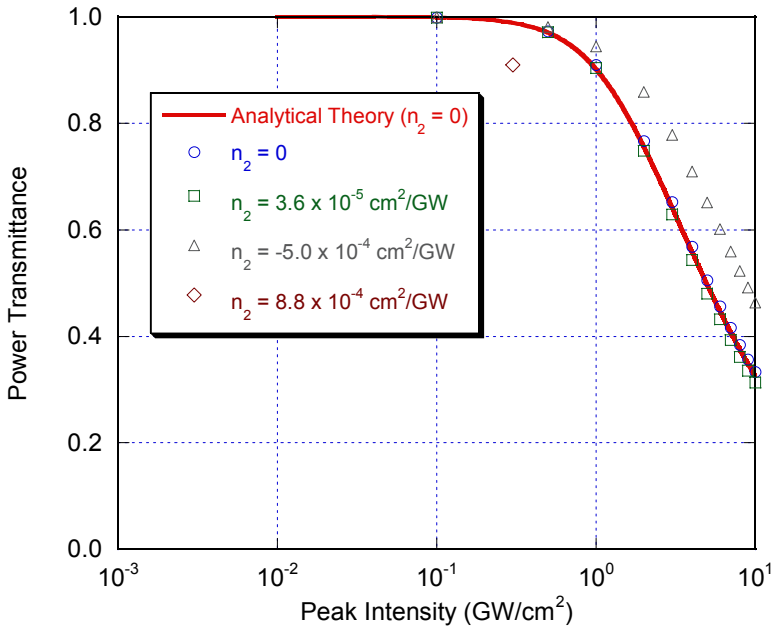

Figure 7. Nonlinear power transmittance vs. peak intensity for a hypothetical material like AF455 but with various values of nonlinear index coefficient.

lytical prediction even at relatively low intensity, as indicated by the single diamond point in Figure 7. It seems unlikely that a third-order effect would contribute such a large nonlinear index, since n_2 is probably due mostly to the solvent at this concentration, and the n_2 for THF is smaller than that of CS_2. However, ESA can make a substantial contribution to the nonlinear refractive index. From the example given in Section 5.2, the index change due to population of the excited state would be $\Delta n \sim 10^{-3}$. This is a substantial index modulation and larger than the one used in the calculation in Figure 7 ($\Delta n = n_2 I = 2.6 \times 10^{-4}$) for which $n_2 = 8.8 \times 10^{-4}$ cm^2/GW was assumed. Thus, it is conceivable that nonlinear refraction due to population redistribution (i.e., the creation of excited state species) may be sufficient to lower the NLT in the small energy regime, making it appear that the medium has larger nonlinear absorption cross sections. Finally, we must

also consider the possibility that both positive and negative index effects (e.g., population redistribution and thermal effects) may be at play simultaneously (with possibly different relative strengths at different pulse energies), affecting the overall shape of the NLT curve. This is only speculative at this point, but plausible based on the above analyses. More work is necessary to characterize these coefficients and test the model.

6. CONCLUSIONS

In summary, we have measured the excited state properties of donor-acceptor push-pull charge-transfer chromophores and modeled the nanosecond NLT as an effective three-photon absorption process combined with stimulated scattering at high intensities. We have also considered the effects due to nonlinear refraction by employing a three-dimensional nonlinear beam propagation model. Several model parameters, including intrinsic TPA cross sections, have been measured independently, and the analytical model shows relatively good agreement with NLT data from solutions for which the molecular TPA and ESA cross sections have been accurately measured. Discrepancies appear when the excited singlet-singlet cross sections are not well determined (i.e., the excited state absorbance measurements are noisy), and smaller discrepancies are also observed in almost every sample, particularly in the low energy region. We have argued that it is unlikely that any of these discrepancies originate from stimulated scattering effects, and that it is plausible that their origin may rooted in nonlinear refraction. We conclude that the dominant contribution to the nonlinear transmission in these chromophores in the nanosecond regime is ESA from singlet states, with only minor contributions from triplet states due to the low triplet quantum yield. TPA does not contribute significantly to the transmittance loss, but is key to pumping the excited states. Nonlinear refraction must be studied in more detail to determine its impact on the NLT at both low and high intensities. Further modeling work is required to properly incorporate nonlinear refraction from population redistribution and thermal effects, and to measure these coefficients in sample solutions.

ACKNOWLEDGEMENTS

We gratefully acknowledge the Air Force Office of Scientific Research (AFOSR/NL) for their support of this work, as well as support from AFRL/ML.

REFERENCES

1. M. Albota, D. Beljonne, J. –L. Brédas, J. E. Ehrlich, J. –Y. Fu, A. A. Heikal, S. E. Hess, T. Kogej, M. D. Levin, S. R. Marder, D. McCord-Maughon, J. W. Perry, H. Röckel, M. Rumi, G. Subramaniam, W. W. Webb, X. –L. Wu, and C. Xu, "Design of organic molecules with large two-photon absorption cross sections," Science **281**, 1653-1656 (1998).
2. B. A. Reinhardt, L. L. Brott, S. J. Clarson, A. G. Dillard, J. C. Bhatt, R. Kannan, L. Yuan, G. S. He, and P. N. Prasad, "Highly active two-photon dyes: Design, synthesis, and characterization toward application," Chem. Mater. **10**, 1863-1874 (1998).
3. M. Rumi, J. E. Ehrlich, A. A. Heikal, J. W. Perry, S. Barlow, Z. Hu, D. McCord-Maughon, T. C. Parker, H. Röckel, S. Thayumanavan, S. R. Marder, D. Beljonne, and J. –L. Brédas, "Structure-property relationships for two-photon absorbing chromophores: bis-donor diphenylpolyene and bis(styryl)benzene derivatives," J. Am. Chem. Soc. **112**, 9500-9510 (2000).
4. R. Kannan, G. S. He, T. –C. Lin, P. N. Prasad, R. A. Vaia, and L. –S. Tan, "Toward highly active two-photon absorbing liquids. Synthesis and characterization of 1,3,5-triazine-based octupolar molecules," Chem. Mater. **16**, 185-194 (2004).
5. J. E. Ehrlich, X. –L. Wu, I. –Y. S. Lee, Z. –Y. Hu, H. Röckel, S. R. Marder, and J. W. Perry, "Two-photon absorption and broadband optical limiting with bis-donor stilbenes," Opt. Lett. **22**, 1843-1845 (1997).
6. R. Kannan, G. S. He, L. Yuan, F. Xu, P. N. Prasad, A. G. Dombroskie, B. A. Reinhardt, J. W. Baur, R. A. Vaia, and L. –S. Tan, "Diphenylaminofluorene-based two-photon-absorbing chromophores with various π-electron acceptors," Chem. Mater. **13**, 1896-1904 (2001).
7. J. Kleinschmidt, S. Rentsch, W. Tottleben, and B. Wilhelmi, "Measurement of strong nonlinear absorption in stilbene-chloroform solution, explained by the superposition of two-photon absorption and one-photon absorption from the excited state," Chem. Phys. Lett. **24**, 133-135 (1974).

8. M. Zhao, Y. Cui, M. Samoc, P. N. Prasad, M. R. Unroe, and B. A. Reinhardt, "Influence of two-photon absorption on third-order nonlinear optical processes as studied by degenerate four-wave mixing: The study of soluble didecyloxy substituted polyphenyls," J. Chem. Phys. **95**, 3391-4401 (1991).
9. R. L. Sutherland, E. Rea, L. V. Natarajan, T. Pottenger, and P. A. Fleitz, "Two-photon absorption and second hyperpolarizability measurements in diphenylbutadiene by degenerate four-wave mixing," J. Chem. Phys. **98**, 2593-2603 (1993).
10. P. Palffy-Muhoray, H. J. Yuan, L. Li, M. A. Lee, J. R. DeSalvo, T. H. Wei, M. Sheik-Bahae, D. J. Hagan, and E. W. Van Stryland, "Measurements of third order optical nonlinearities of nematic liquid crystals," Mol. Cryst. Liq. Cryst. **207**, 291-305 (1991).
11. A. A. Said, C. Wamsley, D. J. Hagan, E. W. Van Stryland, B. A. Reinhardt, P. Roderer, and A. G. Dillard, "Third- and fifth-order optical nonlinearities in organic materials," Chem. Phys. Lett. **228**, 646-650 (1994).
12. R. L. Sutherland, M. C. Brant, J. Heinrichs, J. E. Rogers, J. E. Slagle, D. G. McLean, and P. A. Fleitz, "Excited state characterization and effective three-photon absorption model of two-photon-induced excited state absorption in organic push-pull charge-transfer chromophores," J. Opt. Soc. Am. B **22**, 1939-1948 (2005).
13. D. G. McLean, R. L. Sutherland, J. E. Rogers, J. Slagle, M. Brant, and P. Fleitz, "Interpretation of two-photon-absorption-driven nonlinear absorption," in Nonlinear Optical Transmission and Multiphoton Processes in Organics III, A. T. Yeates, ed., Proc. SPIE **5934**, 593401, 1-15 (2005).
14. F. Gel′mukhanov, A. Baev, P. Macák, Y. Luo, and H. Ågren, "Dynamics of two-photon absorption by molecules and solutions," J. Opt. Soc. Am. B **19**, 937-945 (2002).
15. J. E. Rogers, J. E. Slagle, D. G. McLean, R. L. Sutherland, D. M. Krein, T. M. Cooper, M. Brant, J. Heinrichs, R. Kannan, L. –S. Tan, A. M. Urbas, and P. A. Fleitz, "Development of novel two-photon absorbing chromophores," in Nonlinear Optical Transmission and Multiphoton Processes in Organics IV, A. T. Yeates, ed., Proc. SPIE **6330** (2006).
16. G. S. He, T. –C. Lin, and P. N. Prasad, "Stimulated Rayleigh-Bragg scattering enhanced by two-photon excitation," Opt. Express **12**, 5952-5961 (2004).
17. G. S. He, C. Lu, Q. Zheng, P. N. Prasad, P. Zerom, R. W. Boyd, and M. Samoc, "Stimulated Rayleigh-Bragg scattering in two-photon absorbing media," Phys. Rev. A **71**, 063810 (2005).
18. Y. Silberberg and I. Bar Joseph, "Optical instabilities in a nonlinear Kerr medium," J. Opt. Soc. Am. B **1**, 662-670 (1984).
19. Y. Silberberg and I. Bar Joseph, "Instabilities, self-oscillation, and chaos in simple nonlinear optical interaction," Phys. Rev. Lett. **48**, 1541-1543 (1982).
20. P. Yeh, "Exact solution of a nonlinear model of two-wave mixing in Kerr media," J. Opt. Soc. Am. B **3**, 747-750 (1986).
21. R. Boyd, Nonlinear Optics (Academic Press, New York, 1992).
22. G. S. He, J. Swiatkiewicz, Y. Jiang, P. N. Prasad, B. A. Reinhardt, L. –S. Tan, and R. Kannan, "Two-photon excitation and optical spatial-profile reshaping via a nonlinear absorbing medium," J. Phys. Chem. A **104**, 4805-4810 (2000).
23. R. L. Sutherland, "Energy transfer between incident laser and elastically backscattered waves in nonlinear absorption media," Opt. Express **13**, 9788-9795 (2005).
24. M. D. Feit and J. A. Fleck, Jr., "Simple spectral method for solving propagation problems in cylindrical geometry with fast Fouier transforms," Opt. Lett. **14**, 662-664 (1989).
25. D. I. Kovsh, S. Yang, D. J. Hagan, and E. W. Van Stryland, "Nonlinear optical beam propagation for optical limiting," Appl. Opt. **38**, 5168-5180 (1999).
26. J. E. Rogers, J. E. Slagle, D. G. McLean, R. L. Sutherland, B. Sankaran, R. Kannan, L. –S. Tan, and P. A. Fleitz, "Understanding the one-photon photophysical properties of a two-photon absorbing chromophore," J. Phys. Chem. A **108**, 5514-5520 (2004).
27. E. Parilov and M. Potasek, "Generalized theoretical treatment and numerical method of time-resolved radially-dependent laser pulses interacting with multi-photon absorbers," J. Opt. Soc. Am. B **23**, in press (2006).